

## Small-amplitude excitations in a deformable discrete nonlinear Schrödinger equation

V. V. Konotop\* and M. Salerno†

*Department of Theoretical Physics, University of Salerno, I-84100, Salerno, Italy*

(Received 9 July 1996)

A detailed analysis of the small-amplitude solutions of a deformed discrete nonlinear Schrödinger equation is performed. For generic deformations the system possesses “singular” points which split the infinite chain in a number of independent segments. We show that small-amplitude dark solitons in the vicinity of the singular points are described by the Toda-lattice equation while away from the singular points they are described by the Korteweg–de Vries equation. Depending on the value of the deformation parameter and of the background level several kinds of solutions are possible. In particular, we delimit the regions in the parameter space in which dark solitons are stable in contrast with regions in which bright pulses on nonzero background are possible. On the boundaries of these regions we find that shock waves and rapidly spreading solutions may exist. [S1063-651X(97)01902-8]

PACS number(s): 03.20.+i, 11.10.Lm, 42.65.-k, 43.25.+y

### I. INTRODUCTION

The general discrete nonlinear Schrödinger equation (GDNLS)

$$i\dot{q}_n + (1 + \eta|q_n|^2)(q_{n-1} + q_{n+1} - 2q_n) + 2(\omega_n + |q_n|^2)q_n = 0 \quad (1)$$

was introduced in Ref. [1] as a generalization of the simple tight-binding linear Schrödinger model for the dynamics of quasiparticles in a molecular crystal. In this equation  $q_n$  represents the complex mode amplitude of the molecular vibration at site  $n$ ,  $\omega_n$  is the on-site frequency of the vibration, while the nonlinear terms arise, in the adiabatic and small field approximation, as the result of the interaction of the quasiparticle with the lattice. From a mathematical point of view this system represents a norm preserving deformation of the diagonal discretization of the nonlinear Schrödinger equation (DNLS). The presence of the deformation parameter  $\eta \in \mathbb{R}$  in the system allows one to study, both at the classical and at the quantum level, the interplay between on-site–intersite interactions as well as integrability–nonintegrability and discrete–continuum properties [2–7,9]. For  $\eta=1$  (off-diagonal nonlinearity) the GDNLS reduces to the integrable Ablowitz-Ladik (AL) model with exact soliton solutions while for  $\eta=0$  (on-site nonlinearity) it gives the nonintegrable DNLS system. For intermediate values of  $\eta$  it allows all possible splitting of the nonlinearity among three adjacent sites (equal splitting is at  $\eta=2/3$ ). The properties of the localized mode solutions and of the plane waves (modulational instability) of Eq. (1) were studied in a series of publications [4,5]. Bloch oscillations of bright solitons in the external electric field ( $\omega_n = \gamma n$ ,  $\gamma$  being a constant) at

$\eta=1$  were also considered in [6] and in the case  $0 < \eta \leq 1$  in [7] while the spatial properties and the existence of breath-erlike impurity modes were reported in Refs. [8,9]. All these studies dealt mainly with the attractive case (i.e.,  $\eta > 0$ ) at  $\omega_n = 0$ , in which bright solitary pulses are stable.

The aim of the present paper is to investigate the properties of the small-amplitude solution of the GDNLS equation in the repulsive case  $\eta < 0$ . In the following we refer to this as the stable case since the plane wave solutions corresponding to the center of the Brillouin zone (BZ) are modulationally stable. To this end we consider  $\eta = -\epsilon$  with  $0 < \epsilon < 1$  and fix  $\omega_n = \rho^2$  with  $\rho$  a constant which will be associated with the amplitude of  $q_n$  either at infinity or at the singular points (see below).

The GDNLS is then written as

$$i\dot{q}_n + (1 - \epsilon|q_n|^2)(q_{n-1} + q_{n+1} - 2q_n) + 2(\rho^2 - |q_n|^2)q_n = 0. \quad (2)$$

The inverse scattering technique for Eq. (2) at  $\epsilon=1$  (stable AL) has been developed in [10], its dark soliton solution has been found in [11], and Bloch oscillations of the dark soliton in a constant electric field were reported in [12] [note that we have changed the sign in front to the on-site nonlinearity in Eq. (2) just to have  $\epsilon=1$  as the AL limit].

Though many aspects of the behavior of solutions of Eq. (2) at  $\epsilon=1$  are very similar to the behavior of their counterparts in the continuum limit (see, e.g., [13]) it has been shown in [14,15] that there are drastic differences between the discrete and continuum dynamics when the amplitude of a site excitation approaches one. In this case the dispersive term becomes zero and the given site decouples from its neighbors. It is a direct consequence of the explicit form of Eq. (2) that at  $\epsilon < 1$  a site must have an amplitude  $\rho = \epsilon^{-1/2}$  to become decoupled. When this happens we call the corresponding point a singular point. Thus singular points, splitting the infinite chain in a number of independent segments, exist for the GDNLS for arbitrary nonzero values of the deformation parameter. In the present paper, by performing a multiple scale expansion of the GDNLS around singular points, we show the existence of dark solitons which in the

\*Permanent address: Department of Physics and Center of Mathematical Sciences, University of Madeira, Praça do Município, Funchal, P-9000, Portugal.

Electronic address: konotop@dragoeiro.uma.pt

†Also Istituto Nazionale di Fisica della Materia (INFM) unita' di Salerno. Electronic address: salerno@vaxsa.csied.unisa.it

small-amplitude approximation are described by the Toda-lattice equation. Away from singular points we find that dark solitons can exist in certain regions of parameter space  $(\epsilon, \rho)$  and in the small-amplitude limit are described by solitons of the Korteweg–de Vries (KdV) equation. In addition we find a region in the parameter space in which dark solitons are unstable and bright pulses on nonzero background are stable. On one of the boundaries of this region we find, quite surprisingly, that the system becomes effectively dispersionless and the formation of shock waves becomes possible. The second boundary corresponds to an effectively linear regime where initially localized pulse spreads out quite rapidly. The analytical results, derived in terms of a multiple scale expansion, are found in good agreement with direct numerical simulations of the GDNLS even behind the limit of validity of the small-amplitude approximation.

The paper is organized as follows. In Sec. II we study singular point solutions of the GDNLS by considering the case of a single site between two singular points. In Sec. III we examine small-amplitude dark solitons in the neighborhood of the singular points in terms of the Toda chain. In Sec. IV we consider a multiple scale expansion of the dynamics of chain excitations when the amplitude of the background is less than the amplitude of the singular points. Finally we briefly discuss the regime of zero effective nonlinearity and the possibility of shock wave solutions in the GDNLS. In the conclusions we summarize the main results of the paper.

## II. SINGULAR POINTS AND ONE-SITE DYNAMICS

Let us consider Eq. (2) subject to the nonzero boundary conditions

$$q_n \rightarrow \rho e^{\pm i\vartheta} e^{-ikn + \omega(k)t} \quad \text{at } n \rightarrow \pm\infty, \quad (3)$$

where  $k$  denotes the wave vector from the first Brillouin zone:  $k \in [-\pi, \pi]$ ,  $\omega(k) = 4(1 - \epsilon\rho^2)\sin^2(k/2)$  is the frequency of the background, and  $\vartheta$  is a constant phase. It possesses the following integral of motion:

$$I = \sum_{n=-\infty}^{\infty} \{ \epsilon(q_n \bar{q}_{n-1} + q_{n-1} \bar{q}_n) + 2(1 - \epsilon)(|q_n|^2 - \rho^2) \}. \quad (4)$$

As mentioned above, if at some site  $n$  the amplitude of oscillations is  $\epsilon^{-1/2}$ , and hence

$$q_n = \epsilon^{-1/2} e^{i\omega_0 t - ikn + i\vartheta}, \quad (5)$$

with

$$\omega_0 = 2(\rho^2 - \epsilon^{-1}), \quad (6)$$

the evolution of  $q_{n-1}$  becomes disconnected from  $q_{n+1}$ .

So, for two singular points placed on sites  $l_-$  and  $l_+$  (with  $l_{\pm}$  integers), there is an integral of motion

$$I_{l_-, l_+} = \sum_{n=l_-+1}^{l_+} \{ \epsilon(q_n \bar{q}_{n-1} + q_{n-1} \bar{q}_n) + 2(1 - \epsilon)|q_n|^2 \} \quad (7)$$

associated with the dynamics of the segment between  $l_-$  and  $l_+$ , which naturally follows from Eq. (4).

The integral  $I_{l_-, l_+}$  allows us to find an explicit solution in the case in which one point is placed between two singular points. For the sake of definiteness let us assume that  $l_{\pm} = \pm 1$ , with

$$q_{\pm 1} = \epsilon^{-1/2} \exp(i\omega_0 t \pm i\vartheta) \quad (8)$$

being singular points. Representing the solution of the middle point as

$$q_0 = \epsilon^{-1/2} \nu \exp(i\omega_0 t) \quad (9)$$

one arrives at the following expression for the integral of motion:

$$I_{-1,1} = 2\zeta \cos \vartheta + \frac{1 - \epsilon}{\epsilon} (1 + \zeta^2 + \xi^2). \quad (10)$$

Here  $\zeta$  and  $\xi$  are real and imaginary parts of  $\nu$ :  $\nu = \zeta + i\xi$ . Just from this expression one can see an essential qualitative difference in dynamics of the AL model and GDNLS equation. In the first case [15], i.e., at  $\epsilon = 1$ , there is a region of parameters (at  $|\nu| > 1$ ) where the lattice becomes unstable, this being displayed by an infinite growth of  $\xi$  during finite time. In contrast, even a small value of the difference  $1 - \epsilon$  will prevent this growth. The equations for  $(\zeta, \xi)$  can be obtained from Hamilton's equations with respect to the non-standard Poisson brackets

$$\{f, g\} = [1 - (\zeta^2 + \xi^2)] \left\{ \frac{\partial f}{\partial \zeta} \frac{\partial g}{\partial \xi} - \frac{\partial f}{\partial \xi} \frac{\partial g}{\partial \zeta} \right\}, \quad (11)$$

with respect to the Hamiltonian  $I_{-1,1}$ . Indeed, for  $H = I_{-1,1}$  we have

$$\dot{\zeta} = \{H, \zeta\} = -2 \frac{1 - \epsilon}{\epsilon} [1 - (\zeta^2 + \xi^2)] \xi, \quad (12)$$

$$\dot{\xi} = \{H, \xi\} = 2 \frac{1 - \epsilon}{\epsilon} [1 - (\zeta^2 + \xi^2)] (\Lambda + \zeta), \quad (13)$$

where  $\Lambda = [\epsilon/(1 - \epsilon)] \cos \vartheta$ .

Taking into account the explicit form of  $I_{-1,1}$  one finds a convenient parametrization of the problem as

$$\zeta + \Lambda = R \cos \chi, \quad \xi = R \sin \chi, \quad (14)$$

where  $R$  is a positive constant playing the role of the radius of the orbit in the phase portrait and is related to the energy by

$$R^2 = \frac{\epsilon}{1 - \epsilon} I_{-1,1} + \Lambda^2 - 1. \quad (15)$$

The dynamical equations (12), (13) are easily solved and give the following two different types of orbits.

(a) If  $R < |1 - \Lambda|$  or  $R > |1 + \Lambda|$  (hereafter without restriction of generality we take  $\phi \in [-\pi/2, \pi/2]$ ) the motion is periodic and is governed by the equations

$$\zeta = R \frac{A \cos \Theta - 1}{A - \cos \Theta} + \Lambda, \quad (16)$$

$$\xi = R \sqrt{A^2 - 1} \frac{\sin \Theta}{A - \cos \Theta}, \quad (17)$$

where

$$\Theta = 4 \sqrt{A^2 - 1} R (\cos \vartheta) t + 2 \arctan \left( \frac{\sqrt{A^2 - 1}}{A + 1} \frac{\xi_0}{R + \Lambda + \zeta_0} \right) \quad (18)$$

and

$$A = \frac{1 - R^2 - \Lambda^2}{2\Lambda R} \quad (A^2 > 1). \quad (19)$$

Here  $\xi_0, \zeta_0$  denote the initial values at  $t=0$ .

(b) If  $|1 - \Lambda| < R < |1 + \Lambda|$  the system displays aperiodic motion described by the equations

$$\zeta = -R \frac{A \cosh \Theta - 1}{\cosh \Theta + A} + \Lambda, \quad (20)$$

$$\xi = R \sqrt{1 - A^2} \frac{\sinh \Theta}{\cosh \Theta + A}, \quad (21)$$

where

$$\Theta = 4R \sqrt{1 - A^2} (\cos \vartheta) t + 2 \ln \frac{\xi_0 \sqrt{1 - A^2} + (A + 1)(R + \Lambda + \zeta_0)}{\xi_0 \sqrt{1 - A^2} - (A + 1)(R + \Lambda + \zeta_0)} \quad (22)$$

and the constant  $A$  is given by Eq. (19) (note that now  $A^2 < 1$ ).

The existence of two regimes oscillating and aperiodic is evident from the phase portrait which consists of circles of the radius  $R$  which in the integrable limit  $\epsilon = 1$  degenerates into a straight line. In the aperiodic case a circular trajectory always crosses the unit circle (given by  $|\nu| = 1$ ), the crossing point being just the singular point. Thus for  $|A| < 1$  an initial condition will move on the circle characterized by  $R$  and, as  $t \rightarrow \infty$ , it will reach the singular point on the unit circle. For  $|A| > 1$  there will be no crossing and the point will continue to rotate on the respective circle.

From the above analysis it follows that if initially  $|q_n| \leq \epsilon^{-1}$  (or  $|q_n| \geq \epsilon^{-1}$ ) this will be true for all times. This property is valid also for the integrable AL system [15–17].

### III. SMALL-AMPLITUDE DARK SOLITONS NEAR SINGULAR POINTS

Rather complete description of the dynamics of Eq. (2) is also available for the small-amplitude pulses. Indeed, starting with the case of the excitations slightly deviating from the singular points, we can consider backgrounds for the nonlinear excitations in the form of arbitrary (i.e., with arbitrary  $k$  values in the BZ) set of the singular points. For the sake of simplicity in the present section we restrict the analysis ei-

ther to the center of the BZ,  $k=0$ , or to the edge of the BZ,  $k=\pi$ .

The AL dark soliton ( $\epsilon=1$ ) is written in the form

$$q_n^{\text{AL}}(t) = \rho \left[ 1 - \frac{\sin^2 \vartheta}{\cosh^2(Kn - \Omega t)} \right]^{-1/2} \times \exp[-i \tan \vartheta \tanh(Kn - \Omega t)], \quad (23)$$

with the parameters  $K, \vartheta, \rho$  linked by

$$\sinh \frac{K}{2} = \frac{\rho}{\sqrt{1 - \rho^2}} \sin \vartheta. \quad (24)$$

The phase  $\vartheta$  parametrizes the family of the soliton solutions and is chosen in the interval  $[-\pi, \pi]$ . The small-amplitude limit corresponds to the case  $\vartheta \ll 0$ . In order to expand Eq. (23) around  $\vartheta=0$  we observe that the most natural representation of the solution of the GDNLS equation at  $\epsilon \ll 1$  is

$$q_n = \kappa^n \epsilon^{-1/2} (1 - \gamma^2 \mu a_n) e^{-i \gamma \mu \chi_n + i \omega_0 t}, \quad (25)$$

where  $\gamma \ll 1$  is a small parameter,  $a_n = a_n(\tau)$  and  $\chi_n = \chi_n(\tau)$  are two real functions of the slow time  $\tau = 2\gamma \sqrt{2(\epsilon^{-1} - 1 - \kappa)} t$ , and  $\omega_0$  is given by Eq. (6). The parameter  $\kappa = \pm 1$  introduced in Eq. (25) will be used to choose two different background oscillations, i.e., in-phase oscillations ( $\kappa=1$ ) and out-of-phase oscillations ( $\kappa=-1$ ) corresponding to  $k=0$  and  $k=\pi$ , while the parameter  $\mu = \pm 1$  is used to obtain either dark ( $\mu=1$ ) or bright ( $\mu=-1$ ) pulses.

Substituting Eq. (25) in Eq. (2) and gathering all the terms of orders up to  $\gamma^3$  we arrive at the following Toda system [13]:

$$\frac{da_n}{d\tau} = a_n (c_n - c_{n-1}), \quad (26)$$

$$\frac{dc_n}{d\tau} = a_{n+1} - a_n, \quad (27)$$

where

$$c_n = \sqrt{2|\epsilon^{-1} - 1 - \kappa|} (\chi_n - \chi_{n+1}), \quad (28)$$

and

$$\mu = \kappa \operatorname{sgn}(\epsilon^{-1} - 1 - \kappa). \quad (29)$$

(For the integrable case this system was also obtained in [18].) We have therefore that small-amplitude dark pulses near the singular points can be viewed as exact solitons of the Toda lattice moving on the oscillating background  $\rho \exp(i\omega_0 t)$ . When  $\kappa=1$  ( $k=0$ ), it follows from Eq. (29) that  $\mu=1$ , i.e., the respective solution (25) is always dark, so that its energy profile is always below the background level. On the other hand, at the edge of the BZ we have that  $\kappa=-1$  and the sign of  $\mu$  depends on  $\epsilon$ . We find that  $\mu=1$  for  $\epsilon < 1/2$  and  $\mu=-1$  for  $\epsilon > 1/2$ . This implies that at  $k=\pi$  small-amplitude dark solitons exist for  $\epsilon > 1/2$  while for  $\epsilon > 1/2$  a bright pulse should appear. To check these predictions we have numerically integrated the GDNLS system

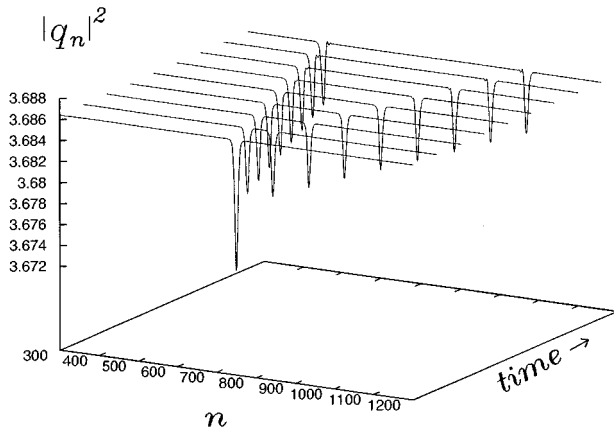


FIG. 1. Time evolution of an initial dark pulse ( $\mu=1$ ) on an in-phase background ( $\kappa=1$ ) at  $\epsilon=0.25$ . The total integration time is 300. The initial condition corresponds to a soliton of the Toda lattice.

with a fifth-order Runge-Kutta adaptive step-size algorithm (the numerical error was controlled by checking the conservation of the norm up to the fifth decimal digit). In Fig. 1 the time evolution of a small-amplitude dark soliton on a line of 1500 sites with an in-phase ( $\kappa=1$ ) background is reported. Here the initial condition is of the form of a one-soliton solution of the Toda lattice which corresponds to a bisoliton solution of the GDNLS. We see that the initial pulse splits in two dark excitations which are stable over long time. This is in contrast with what happens for a bright profile on the same background and for the same parameter values as reported in Fig. 1. This behavior is found to be true for all values of  $\epsilon$  in the range  $(0,1]$ . The same analysis, but for an out-of-phase background ( $\kappa=-1$ ), shows that bright pulses are stable and dark ones are unstable if  $\epsilon < 1/2$ , while dark pulses are stable and bright ones are unstable if  $\epsilon > 1/2$ . In Figs. 2 and 3, we have reported the evolution of a bright and dark GDNLS bisoliton for  $\epsilon$  values, respectively, at  $\epsilon=0.25$  and  $\epsilon=0.75$ . We see that the pulses are quite stable, in agreement with our predictions. From the above analysis it is also clear that at the ‘‘critical’’ value  $\epsilon=1/2$  the solution changes sta-

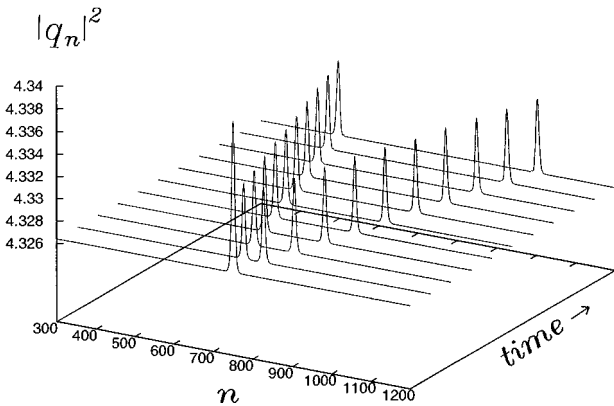


FIG. 2. Time evolution of an initial bright ( $\mu=-1$ ) pulse on an out-of-phase background ( $\kappa=-1$ ) at  $\epsilon=0.25$ . The total integration time is 300. The initial condition corresponds to a soliton of the Toda lattice.

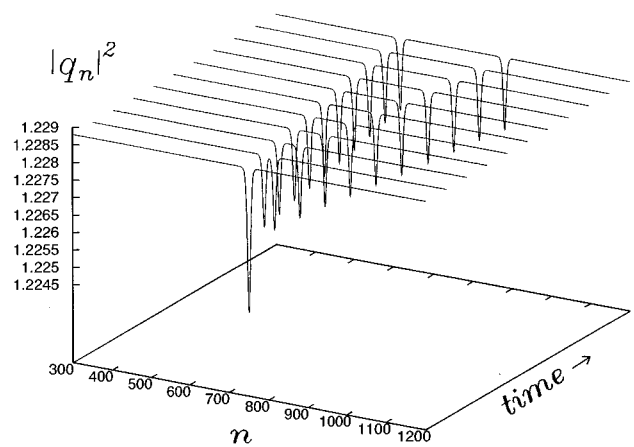


FIG. 3. Same as in Fig. 2 but for a dark initial condition at  $\epsilon=0.75$ .

bility and the dynamics manifests a strong dispersive character (weakly nonlinear or effectively linear regime). In Figs. 4 and 5 the time evolution of a bisoliton, respectively, dark and bright, at the ‘‘critical’’ value  $\epsilon=1/2$  is reported. We see that in both cases the profiles decay in background radiation in agreement with our prediction.

#### IV. SMALL-AMPLITUDE EXCITATIONS FAR FROM THE SINGULAR POINTS AND SHOCK WAVES OF THE GDNLS

In order to find dynamical equations for small-amplitude pulses far from the singular points we apply the same analysis as in the preceding section but now we expand around

$$q_n = [\rho + a_n(t)] e^{-i\Phi_n(t)}, \quad (30)$$

where

$$a_n(t) = \gamma^2 a^{(0)}(T, X; \tau) + \gamma^4 a^{(1)}(T, X; \tau) + \dots, \quad (31)$$

$$\Phi_n(t) = \gamma \Phi^{(0)}(T, X; \tau) + \gamma^3 \Phi^{(1)}(T, X; \tau) + \dots \quad (32)$$

In the above expansion  $X = \gamma n$ ,  $T = \gamma t$  denote fast space and time variables while  $\tau = \gamma^3 t$  represents a slow time. By

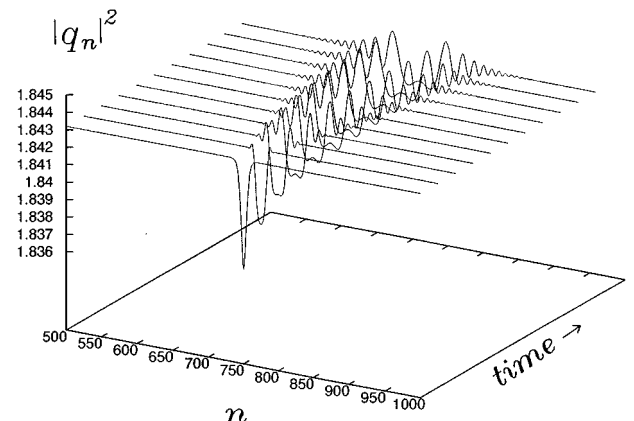


FIG. 4. Time evolution of an initial dark pulse ( $\mu=1$ ) on an out-of-phase background ( $\kappa=-1$ ) at the critical value  $\epsilon=0.5$ . The total integration time is 1200.

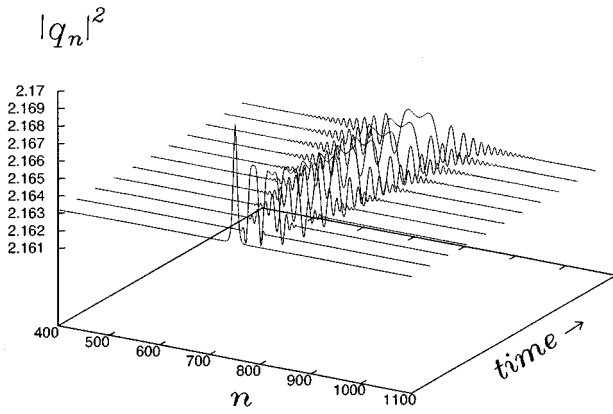


FIG. 5. Same as in Fig. 4 but for a bright pulse ( $\mu = -1$ ).

analyzing the equations of all orders from  $\gamma$  up to  $\gamma^5$  we find that at the leading orders ( $\gamma^2, \gamma^3$ ) the GDNLS system reduces to

$$\frac{\partial \Phi^{(0)}}{\partial T} = 4\rho^2 a^{(0)}, \quad (33)$$

$$\frac{\partial a^{(0)}}{\partial T} = (1 - \epsilon\rho^2) \frac{\partial^2 \Phi^{(0)}}{\partial X^2}. \quad (34)$$

From system (33), (34) it readily follows that the excitation at leading order moves with the velocity

$$V_\epsilon = -2\rho\sqrt{1 - \epsilon\rho^2} \quad (35)$$

(the given sign of the velocity is chosen only for the sake of convenience), which depends on the background level.

It is of interest to note that the velocity  $V = \Omega/K$  of the AL dark soliton in the small-amplitude limit takes the form

$$V = V_0 + \frac{\partial^2 \rho}{3\sqrt{1 - \rho^2}} (3 - 4\rho^2), \quad (36)$$

where  $V_0$  is given by Eq. (35) at  $\epsilon = 1$  and coincides with the velocity of linear waves against the background  $\rho$  in the long wavelength limit (i.e., in the center of the BZ). It also follows from Eq. (36) that  $V$  coincides with the velocity of the linear waves when  $\rho^2 = 3/4$ .

In the next two orders in  $\gamma$  we obtain the equations

$$\frac{\partial \Phi^{(1)}}{\partial T} - 4\rho^2 a^{(1)} = -\frac{\partial \Phi^{(0)}}{\partial \tau} - (1 - \epsilon\rho^2) \frac{\partial^2 a^{(0)}}{\partial X^2} + 6\rho^2 a^{(0)2}, \quad (37)$$

$$\begin{aligned} \frac{\partial a_n^{(1)}}{\partial T} - (1 - \epsilon\rho^2) \frac{\partial^2 \Phi^{(1)}}{\partial X^2} \\ = -\frac{\partial a^{(0)}}{\partial \tau} + \frac{1}{12} \frac{\partial^3 a^{(0)}}{\partial T \partial X^2} \\ - (2 - 5\epsilon\rho^2) \left( \frac{4\rho^2}{V_\epsilon} \right) a^{(0)} \frac{\partial a^{(0)}}{\partial X}. \end{aligned} \quad (38)$$

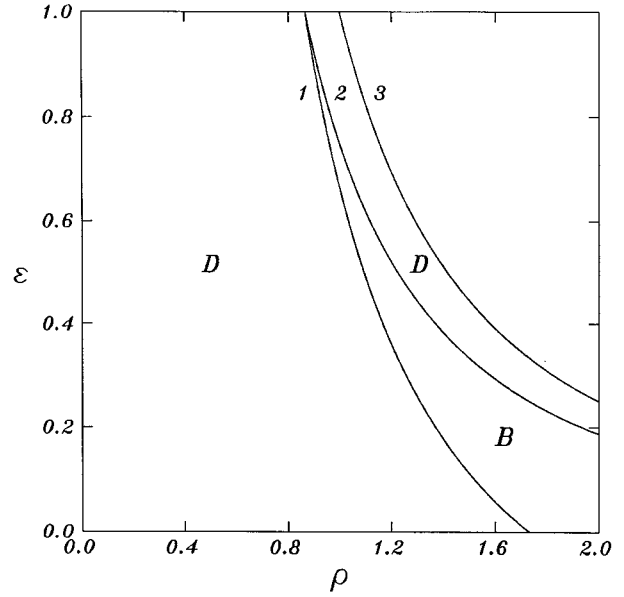


FIG. 6. Parameter space ( $\epsilon, \rho$ ). The window where bright pulses against a nonzero background exist is bounded by the curves (1)  $\epsilon = 1/\rho^2 - 1/3$  and (2)  $\epsilon = 3/(4\rho^2)$ . The curve (3),  $\epsilon = 1/\rho^2$ , corresponds to the singular points and in its vicinity the small-amplitude excitations of the system are governed by the Toda-lattice equation.

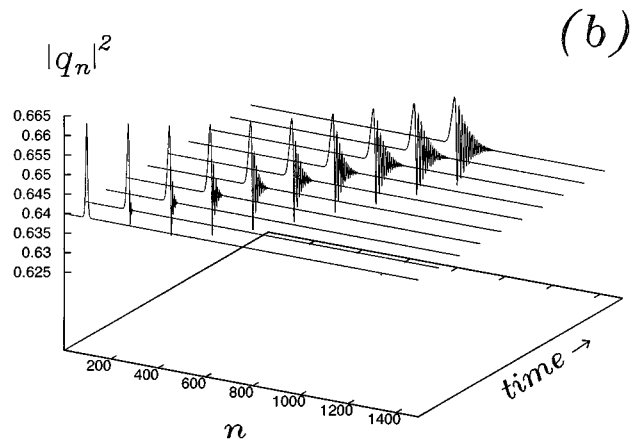
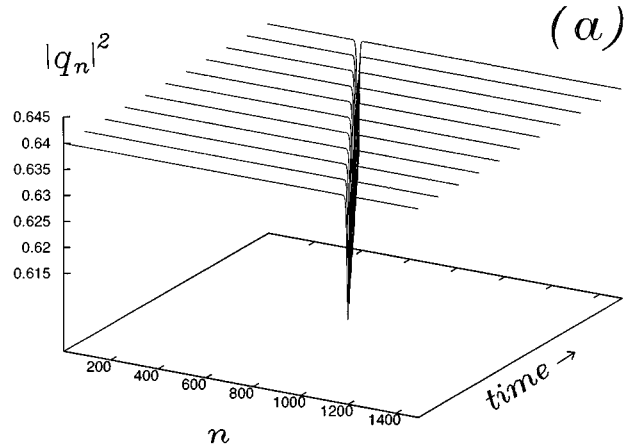


FIG. 7. (a) Time evolution of an initial dark pulse corresponding to a KdV soliton for parameter values  $\epsilon = 0.4, \rho = 0.8$ . (b) Same as in (a) but for initial bright pulse. The total integration time is  $T = 1200$ .

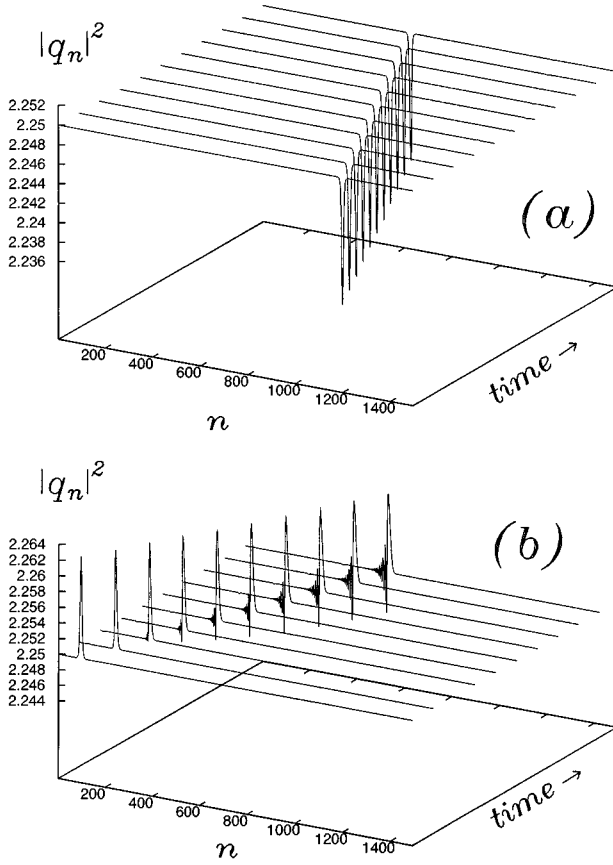


FIG. 8. (a) Time evolution of an initial dark pulse for parameter values  $\epsilon=0.4, \rho=1.5$ . (b) Same as in (a) but for an initial bright pulse. The total integration time is  $T=1200$ .

It is remarkable that the compatibility condition of these two equations directly leads to the following KdV equation:

$$-4\rho\sqrt{1-\epsilon\rho^2}\frac{\partial a^{(0)}}{\partial\tau} - \frac{1}{3}(1-\epsilon\rho^2)[3-(3\epsilon+1)\rho^2]\frac{\partial^3 a^{(0)}}{\partial Z^3} + 8\rho^2(3-4\epsilon\rho^2)a^{(0)}\frac{\partial a^{(0)}}{\partial Z} = 0, \quad (39)$$

where  $Z$  denotes the running variable  $Z=X-V_\epsilon T$ . We remark that a similar result was also obtained in Refs. [5,19].

Equation (39) allows soliton solutions corresponding both to positive and negative  $a^{(0)}$  depending on the sign of the prefactors in the dispersive and nonlinear terms. The results of the respective analysis are illustrated in Fig. 6. In this figure the region between the curves 1 and 2 marked with  $B$  corresponds to parameter values for which stable propagation of bright solitons against the background is possible. In this region dark solitons will not be stable and they will decay in background radiation. The line 3 itself determines the amplitude of the singular points:  $\epsilon=1/\rho^2$ . Close to this line the dynamics of small-amplitude excitations follows Toda equations as described in Sec. II. The areas marked with  $D$  in Fig. 6 correspond to parameter regions in which dark solitons are stable while bright ones are unstable. On curve 2 of Fig. 6 [ $\epsilon=3/(4\rho^2)$ ] the nonlinear term becomes zero as is evident from Eq. (39). This implies that any local-

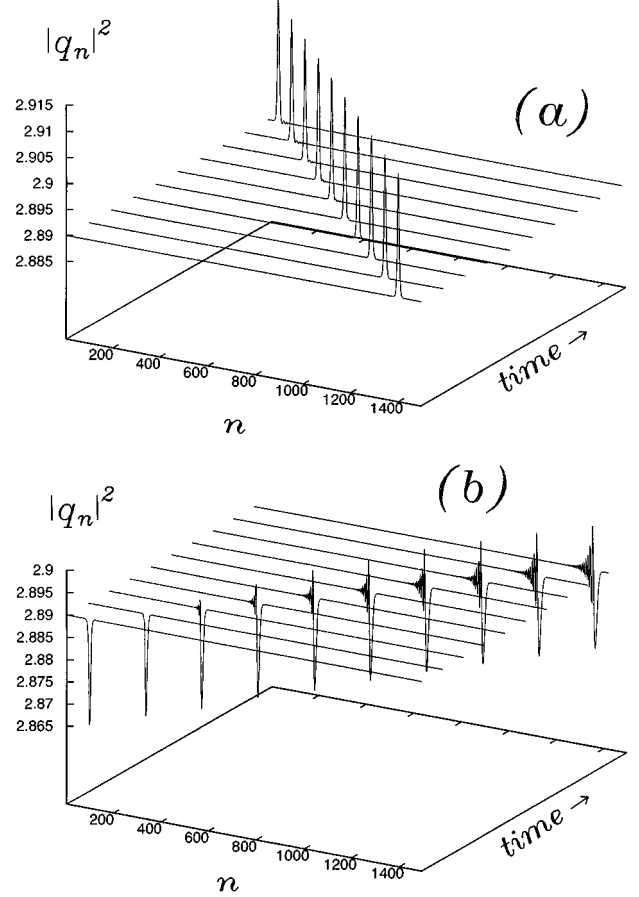


FIG. 9. (a) Time evolution of an initial bright pulse for parameter values  $\epsilon=0.16, \rho=1.7$ . (b) Same as in (a) but for an initial dark pulse. The total integration time is  $T=1200$ .

ized pulse will spread out in background radiation (no solitonlike excitations). On the other hand, on curve 1 of Fig. 6, which represents the other dark-bright interface, the system has different dynamical properties since it becomes effectively dispersionless, it is seen from Eq. (39). Since the nonlinearity on this curve is not zero we expect this case to give shock solutions (see below).

To check these results we have numerically computed the time evolution of small-amplitude bright and dark excitations for parameter values taken in different regions of Fig. 6. In Fig. 7(a) the evolution of a dark soliton at  $\epsilon=0.4, \rho=0.8$  is reported. In Fig. 7(b) we show the same evolution but for an initially bright pulse for the same parameter values as in Fig. 7(a). From these figures it is clear that parameter values on the left of curve 1 correspond to stable dark pulse propagation and to decaying bright excitations. A similar behavior is found in the region between curve 2 and curve 3. This is seen from Figs. 8(a) and 8(b) in which the evolution of, respectively, a dark and a bright excitation is reported at parameter values  $\epsilon=0.4, \rho=1.5$ . In the region between curve 1 and curve 2 the behavior is just the opposite, i.e., dark solitons decay in background radiation while bright pulses can propagate as solitary waves. This is shown in Figs. 9(a) and 9(b) for, respectively, a bright and a dark initial profile at parameter values  $\epsilon=0.16, \rho=1.7$ . It is of interest to remark that while for the pulses of Fig. 7(b), the radiation is on the front,

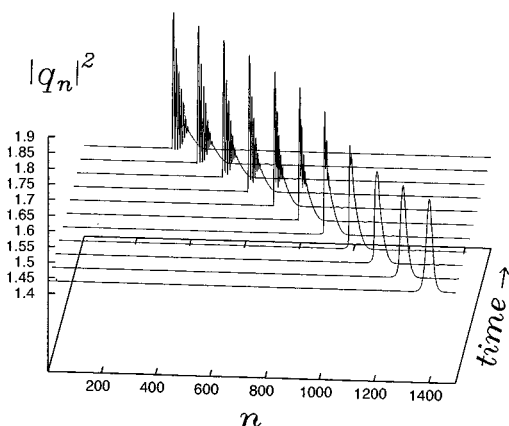


FIG. 10. Shock wave formation from a smooth bright pulse at parameter values  $\epsilon=0.361(1)$ ,  $\rho=1.2$  on curve 1 of Fig. 6. The total integration time is  $T=1200$ .

in Figs. 8(b) and 9(b) the radiation is just on the back. This corresponds to the fact that wave packets in the region on the left of curve 1 always have group velocity greater than the velocity  $V_\epsilon$  of the background radiation while the opposite is true for the complementary regions.

From Eq. (39) it is evident that for  $\epsilon=1/\rho^2-1/3$  the dispersion disappears and the resulting equation possesses shock wave solutions. This surprising property of the GDNLS system has been numerically checked in Fig. 10. In this figure the time evolution of an initial bright profile is reported for parameter values taken on curve 1 of Fig. 6 at  $\epsilon=0.361(1)$ ,  $\rho=1.2$ . We see that the smooth initial profile is distorted with the top moving at higher velocity than the bottom part of the profile. This gives rise to a forward bending of the profile with breaking of the wave and rapid oscillations on the wave front. A similar behavior is observed also

for dark pulses as will be reported in more extended form elsewhere [20]. We should mention that the possibility of shock waves in other chains was also reported in Ref. [21].

## V. CONCLUSION

We have analyzed the properties of the small-amplitude solutions of the GDNLS. Like the well-known AL model the GDNLS equation has singular points for all  $\epsilon$  different from zero which provide effective decoupling of the chain. In this sense one can speak about the dominant role of the nonlinearity of the ‘‘AL type’’ in the behavior of the system. In the meantime, the properties of the singular points are essentially different in the cases  $\epsilon=1$  and  $\epsilon<1$ .

The small-amplitude excitations against constant amplitude backgrounds are governed by the Toda-lattice equation if they are in the vicinity of the singular points or by the KdV equation if the background amplitude is less than  $1/\sqrt{\epsilon}$ . The type of solution essentially depends not only on the deformation parameter but also on the chosen point in the BZ. Existence of the bright pulses against nonzero background above singular points is a nontrivial qualitative demonstration of the mentioned differences. We have delimited the regions in the parameter space in which dark solitons are stable in contrast with regions in which bright pulses on nonzero background are. On the boundaries of these regions we have found, quite surprisingly, that shock waves may exist.

## ACKNOWLEDGMENTS

V.V.K. thanks the Department of Theoretical Physics of the University of Salerno for the warm hospitality. Financial support from INTAS Grant No. 93-1324 and from INFN unita’ di Salerno is also acknowledged.

- 
- [1] M. Salerno, Phys. Rev. A **46**, 6856 (1992).  
 [2] M. Salerno, Phys. Lett. A **162**, 381 (1992).  
 [3] V.Z. Enol’skii, M. Salerno, A.C. Scott, and J.C. Eilbeck, Physica D **59**, 1 (1992).  
 [4] D. Cai, A. R. Bishop, and N. Gronbech-Jensen, Phys. Rev. Lett. **72**, 591 (1994).  
 [5] Yu.S. Kivshar and M. Salerno, Phys. Rev. E **49**, 353 (1994).  
 [6] V.V. Konotop, O.A. Chubykalo, and L. Vázquez, Phys. Rev. E **48**, 563 (1994).  
 [7] D. Cai, A.R. Bishop, N. Gronbech-Jensen, and M. Salerno, Phys. Rev. Lett. **74**, 1186 (1995).  
 [8] D. Henning, N.G. Sun, H. Gabriel, and G.P. Tsironis, Phys. Rev. E **52**, 255 (1995).  
 [9] D. Henning, K.O. Rasmussen, G.P. Tsironis and H. Gabriel, Phys. Rev. E **59**, R4628 (1995).  
 [10] V.E. Vekslerchik and V.V. Konotop, Inverse Problems **8**, 889 (1992).  
 [11] V.V. Konotop and V.E. Vekslerchik, J. Phys. A **25**, 4037 (1992).  
 [12] V.V. Konotop, Teor. Mat. Fiz. **99**, 413 (1994).  
 [13] See, for example, L.D. Faddeev and L.A. Takhtajan, *Hamiltonian Methods in the Theory of Solitons* (Springer, Berlin, 1987).  
 [14] I.T. Khabibulin and A.G. Shagalov, Teor. Mat. Fiz. **83**, 323 (1990).  
 [15] O.A. Chubykalo, V.V. Konotop, L.Vázquez, and V.E. Vekslerchik, Phys. Lett. A **169**, 359 (1992).  
 [16] V.E. Vekslerchik, Phys. Lett. A **174**, 285 (1993).  
 [17] A.K. Common and S.T. Hafez, J. Phys. A **23**, 455 (1990).  
 [18] O.A. Chubykalo, V.V. Konotop, and L. Vázquez, Phys. Rev. B **47**, 7971 (1993). (The small-amplitude expansion in this paper has not taken into account the dispersion of the leading-order system in the case of a soliton far from the singular points. In the present paper we improve the respective result.)  
 [19] Yu.S. Kivshar, Phys. Rev. A **42**, 1757 (1990).  
 [20] V.V. Konotop and M. Salerno (unpublished).  
 [21] B.L. Holian and G.K. Straub, Phys. Rev. B **18**, 1593 (1978); B.L. Holian, H. Flaska, and D.W. McLaughlin, Phys. Rev. A **24**, 2595 (1981); J. Hietarinta, T. Kuusela, and B.A. Malomed, J. Phys. A **28**, 3015 (1995); P. Poggi, S. Ruffo, and H. Kantz, Phys. Rev. E **52**, 307 (1995).